Physicochem. Probl. Miner. Process., 61(1), 2025, 199872

http://www.journalssystem.com/ppmp

Physicochemical Problems of Mineral Processing

ISSN 1643-1049

Application of organic ellagic acid as a selective inhibitor of calcite in scheelite flotation

Yu Wu [1], Xiaokang Li [1], Ying Zhang [1,2], Zhenhao Guan [1], Qingrui He [1]

[1] 1Faculty of Land and Resources Engineering, Kunming University of Science and Technology, Kunming 650093, China

[2] State Key Laboratory of Clean Utilization of Complex Non-Ferrous Metal Resources, Kun-ming University of Science and Technology, Kunming 650093, China

Corresponding author: zhyingcsu@163.com

Abstract: Calcite and scheelite have the same active particles and similar crystal structure, and the flotation behavior is similar. In this paper, a kind of organic ellagic acid (EA) with low molecular weight and high stability was studied as a new environmental inhibitor of low dose calcite. The microflotation test results show that when the dosage of EA is 8 mg/L and NaOL is 30 mg/L, the recovery rate of calcite is 6.22% and the recovery rate of scheelite is 89.35%, which has obvious inhibition effect on calcite. By zeta potential evaluation and Fourier transform, the surface of calcite galena reduces its hydrophobicity and hinders the adsorption of collector. X-ray photoelectron spectroscopy (XPS) and density functional theory (DFT) analysis show that EA occurs mainly through the interaction of -OH and C=O hydrophilic groups with calcium atoms on the surface of calcite, forming Ca-O-C bonds leading to stable adsorption. New, efficient and environmentally friendly organic inhibitors are designed to selectively change the surface properties of calcite and enhance the flotation efficiency of scheelite and calcite.

***Keywords*:** scheelite, calcite, novel depressants, ellagic acid, flotation separation

1. Introduction

Tungsten metal finds extensive applications in alloys, electronics, and the chemical industry owing to its exceptional hardness, high melting point, and density. As a rare and vital metal resource, tungsten plays a crucial role in various sectors (Jiao et al., 2019). With the gradual exploitation of wolframite resources, scheelite ($CaWO_4$), characterized by its "poor, fine, miscellaneous" nature, has emerged as a significant tungsten source. Flotation stands out as a primary production method for scheelite enrichment. The surface chemistry of scheelite is similar to that of gangue mineral calcite, which brings great challenges to the separation of scheelite. Sodium oleate (NaOL) and benzohydroxamic acid (BHA) are widely used collectors in tungsten flotation. The lead complex of benzohydroxamic acid (Pb-BHA) has excellent selective harvesting performance for separating scheelite from calcite and fluorite. Zhao analyzed the structure of Pb-BHA complex by establishing a single crystal - liquid phase - solid/liquid interface analysis method, which helped to reveal the true adsorption structure of the collector. A multi-ligand-MOF (ML-MOF) collector was also formed by molecular design to enhance the trapping capacity and hydrophobicity of Pb-BHA structure (Wei et al., 2023a; Wei et al., 2024). NaOL has good collecting performance of scheelite and calcite. The mechanism of action is that fatty acid ions and Ca^{2+} combine to form fatty acid calcium precipitate, which enhances the hydrophobicity of mineral surface and makes mineral float. Due to its strong harvesting and low selectivity (Guan et al., 2024a), the addition of selective inhibitors is the key to enhance the surface contrast between scheelite and calcium-bearing gangue minerals. Presently, inorganic depressants like sodium silicate are prevalent in scheelite flotation applications. However, their efficacy is susceptible to pH variations, and their high dosage hampers further advancements (Wei et al., 2023b; Guan et al., 2022).

The identification of biological organic matter represents a notable breakthrough in the targeted flotation separation of scheelite and calcite. These compounds, containing polar groups such as -OH

and -COOR, function as depressants by forming chelates with the Ca^{2+} active sites on calcite surfaces (Peng et al., 2024; Yao et al., 2023; Zhu et al., 2019). Offering straightforward design, synthesis, and abundant sources, they are environmentally friendly, being non-toxic and easily degradable. As a result, they hold potential as greener and safer alternatives in mineral processing. Recent research has explored a range of organic depressants, including carboxymethyl cellulose, humic acid, sodium polyacrylate, tartaric acid, and citric acid (Dong et al., 2019; Dong et al., 2023; Zhang et al., 2018; Ai et al., 2018; Wang et al., 2018). However, the solubility of macromolecular organic depressants in solution is limited, posing challenges in reagent preparation. While small molecule depressants like citric acid have shown effectiveness in depressing fluorite, their low polar group content leads to subpar performance in depressing calcite (Yao et al., 2023). Additionally, tartaric acid requires complexation with metal ions to achieve a certain level of depressant effectiveness on calcite (Dong et al., 2021). Hence, there is a pressing need to continue developing efficient and selective flotation depressants for the successful separation of scheelite and calcite.

Ellagic acid (EA) is a natural polyphenol dilactone organic compound widely found in various plant tissues like soft fruits and nuts. Its chemical formula is $C_{14}H_6O_8$, with a molecular weight of 302.28. The structural unit of EA is depicted in Fig. 1 featuring four hydroxyl groups and two lactones, which constitute the hydrophilic region of the molecule. These components exhibit diverse bioactive functions, including antioxidant, anticancer, and anti-mutation properties. EA exerts its protective effect against oxidative stress by chelating with metal ions, a process mainly utilized in the medical industry (Rois et al., 2018; Agrawal and Kulkarni 2020). Due to its abundance of -OH and -COOR functional groups, EA holds potential as a flotation reagent in beneficiation processes. However, its depressant effects in flotation have been scarcely studied. Based on this, this paper used EA as inhibitor to carry out scheelite and calcite flotation tests. The study aims to determine the optimal conditions for scheelite and calcite separation using EA depressant through micro-flotation testing. It would be beneficial to include preliminary results or hypotheses regarding the adsorption mechanism to provide a foundation for the detailed analysis presented.

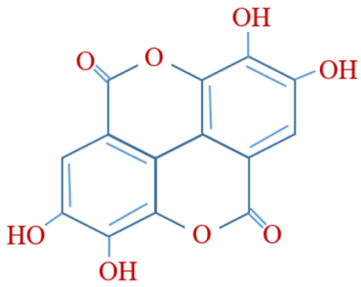

Fig. 1. Chemical structure of EA

2. Experimental

2.1. Minerals

Scheelite and calcite purchased in the test are high purity minerals. After the mineral is broken, the impurities are removed manually, and then ground to -74 μm, and screened to obtain different particle sizes. The microflotation test selects -74+38 μm particle size and -38 μm particle size as samples for other tests, in particular, the Zeta potential test needs to select -5 μm sample. A portion of high purity raw ore was sliced and processed into a cube sample (0.8*0.8*0.3 cm) for contact Angle test and atomic force microscopy (AFM).

XRD analysis was conducted to ascertain the purity of the mineral samples. The test outcomes, depicted in Fig. 2, reveal diffraction peaks corresponding to the crystalline structures of scheelite and calcite. Complemented by the multi-element analysis presented in Table 1, scheelite purity is determined to be 99.16%, while calcite purity stands at 97.7%. The presence of minor impurities such as Si, Mg, etc., is observed, yet remains within acceptable limits as per test requirements. All tests were conducted with deionized water (18.25 MΩ·cm), pH adjusted by HCl and NaOH. EA was obtained from Shanghai Huayuan Century Co., Ltd., with a purity of 98%. NaOL originated from Tianjin Guangfu Fine Chemical Research Institute.

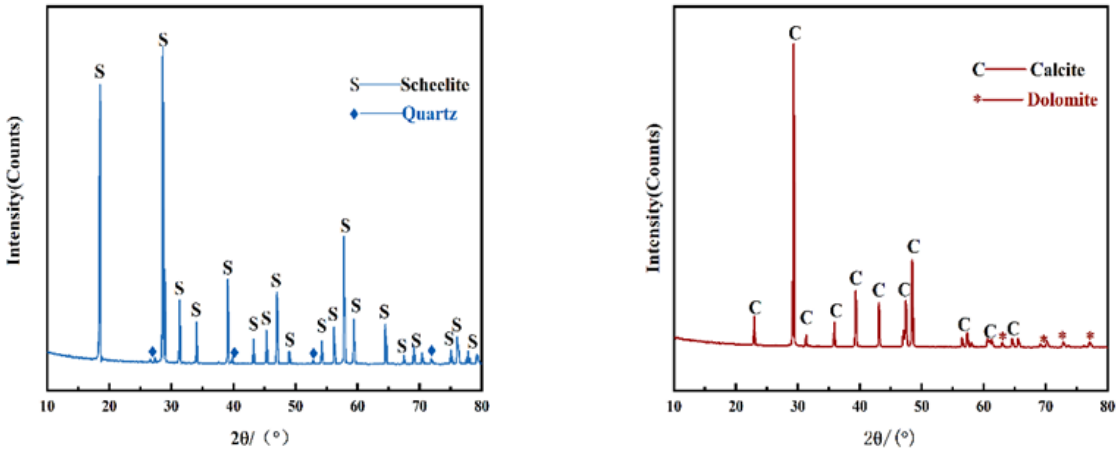

Fig. 2. XRD patterns of scheelite and calcite

Table 1. Mineral multielement analysis table

Minerals	main components %			
	CaO	WO_3	MgO	SiO_2
Scheelite	13.09	79.85	-	0.28
Calcite	54.70	-	0.30	-

2.2. Microflotation test

The pure mineral flotation experiment uses FGC aerated hanging tank flotation machine, equipped with 40mL plexiglass flotation cell. The flotation test was carried out at a stirring speed of 1600 r/min and an air flow rate of 15 m^3/min. 2 g of pure minerals and 38 ml of water were added to the flotation cell for each test. The specific test process is shown in Fig. 3. The pulp is stirred for 1min, the pH of the pulp is adjusted for 3min, the action of EA and NaOL is 3min, and the air is inflated and the bubble is scraped for 3 minutes. Each set of tests was repeated 3 times, and the standard deviation was used to represent the error value. The tailings collected from the flotation cell and the concentrates gathered from the foam undergo filtration, drying, and subsequent weighing. The single mineral recovery (ε) is obtained by formula 1 for the weights of concentrate (M1) and tailings (M2).

$$\varepsilon = \frac{M1}{M1+M2} \times 100\% \quad (1)$$

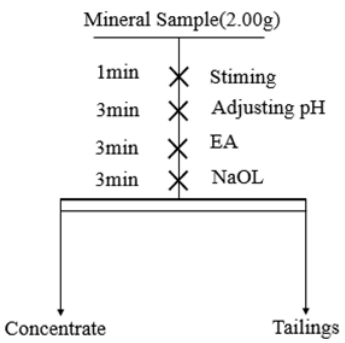

Fig. 3. Microflotation process of pure minerals

2.3. Characterization method

The adsorption capacity test used UV-2700 ultraviolet visible spectrophotometer to scan the full spectrum of different concentrations of EA standard solution. The corresponding characteristic peak wavelength (λ) of EA was determined to be 253.4nm, and the absorbance value was determined. The concentration of EA after absorption was measured by the calibration curve (Fig. 4), and the adsorption amount was calculated according to the change of EA concentration (Formula 2).

$$\tau = (C_0 - C)V/mA \quad (2)$$

Here, τ is the adsorption density, mg/m²; C_0 is the reagent concentration before action, mg/L; C is the reagent concentration after action, mg/L; V is the volume of solution, L; m is the sample weight, g; A is the specific surface area of mineral particles, m²/g. scheelite is 0.2533 m²/g, calcite is 0.2597 m²/g.

Zeta potential is measured using the Zetasizer Nano Zs90 potentiometer (Malvern, UK). The mineral sample (20 mg) was mixed with deionized water (40 mL) and the magnetic stirrer was rotated at 1200 r/min for 1 min to disperse the homogenized pulp. Flotation reagent was added according to the flotation process, the reaction time was 3 min, and after standing for 5 min, appropriate suspension was taken to determine Zeta potential, and the final result was averaged.

Fourier transform infrared spectroscopy (FT-IR) was conducted using the Bruker Alpha infrared spectrometer. Stir 2 g of sample with 40 ml of deionized water and adjust the optimal ph. The quantitative reagent was then added and stirred for a period of 15 minutes, the sample was filtered and dried, and the infrared test was performed.

XPS test uses the PHI 5000 Versaprobe-II device to analyze the changes of chemical element composition on mineral surface under different chemical regimes. Multipak software was used to analyze the test data with 284.8 ev carbon peak of c1s as the reference point of binding energy.

The surface wettability of the mineral samples was tested using a JY-82 contact angle analyzer. Sandpaper was used to polish the mineral slices, which were then cleaned with ethanol. Sand the surface of the slice smooth, and then the slice into the water medium, in order to add a certain amount of reagents reaction for 5 minutes. The slices are removed and the surface is dried for testing.

Atomic force microscopy (AFM) serves as a surface characterization method for evaluating the extent of chemical adsorption on mineral surfaces through imaging. The Bruker Dimension Icon instrument was used to test the mineral in a region of 5 μm × 5 μm, and 2D and 3D images were obtained under different conditions.

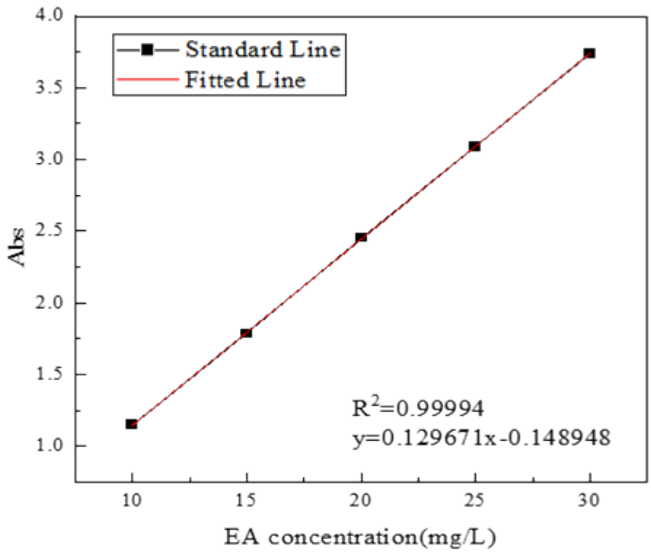

Fig. 4. Relationship between the EA concentration and absorbance

2.4. DFT calculation

The DFT calculation of the adsorption system between calcite crystal and EA reagent was carried out using the CASTEP module of MaterialStudio 2023. Adsorption energy serves as a pivotal indicator of the agent's bonding strength to the mineral surface, reflecting its affinity towards it (Formula 3). A high absolute value of energy indicates that the spontaneous chemical reaction between the agent and the mineral is intense (Yi et al., 2018).

$$E_{ads} = E_{system} - (E_{adsorbate} + E_{surface}) \quad (3)$$

Here E_{ads} denotes the adsorption energy of the adsorbate on the mineral, E_{system} represents the total energy of the adsorption system, $E_{adsorbate}$ signifies the energy of the adsorbate, and $E_{surface}$ indicates the energy of the mineral surface. Detailed optimization parameters are shown in Table 2.

Table 2. Related parameters of CASTEP optimization.

Parameter	Value
Electronic exchange correlation	Ernzerhof (PBE)
Electronic interaction	USPP
Plane wave energy cutoff	571.4 eV
K-point grid	(2 × 2 × 1)
Calculation method	Reverse BFGS algorithm
Self-consistent energy tolerance of the electronic minimizer	2.0×10^{-6} eV/atom
Convergence parameters for energy, maximum force, and maximum displacement	1.0×10^{-5} eV/atom, 0.05 eV/Å, 0.002 Å

3. Results and discussion

3.1. Microflotation test

Fig. 5 (A) shows the flotation effect under different pH conditions. Sodium oleate dosage was determined to be 20mg/L, the optimal pH was 9, and the recoveries of scheelite and calcite were 87.34% and 92.16%. Fig. 5 (B) shows the flotation effect of sodium oleate with different dosage. When the amount of NaOL is 30 mg/L, the recovery rates of scheelite and calcite are 93.05 and 95.73%, respectively, achieving a good collection effect. Therefore, NaOL was determined to be 30mg/L and subsequent tests were carried out.

Fig. 5 (C) shows the effect of EA on the flotation behavior of scheelite and calcite under different pH conditions. Under fixed conditions with EA of 8 mg/L and NaOL of 30 mg/L, the pH range is 6-11. In the highly alkaline slurry environment, scheelite and calcite gradually showed a certain inhibition phenomenon. When pH=11, scheelite recovery decreased to 74.71% and calcite recovery to 5.82%. The best results show that when pH = 8, the recovery of scheelite is 89.35% and calcite is 6.22%, and the difference is 81.13%. Therefore, pH = 8 was determined for the subsequent dosage test.

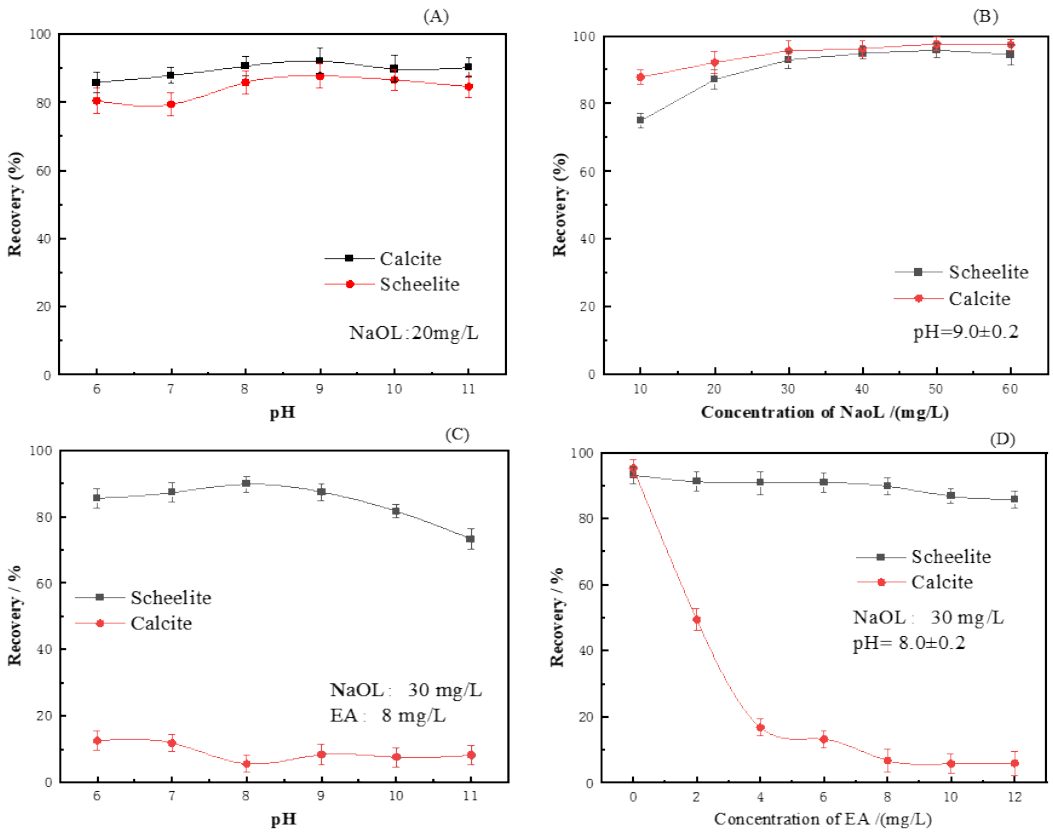

Fig. 5. Effects of pH and chemical concentration on the flotation performance of two minerals

Fig. 5 (D) shows the effect of EA dose on calcite. When the amount of EA is 0mg/L, the recovery of scheelite and calcite is more than 93%. With the increase of EA dosage, the recovery rate of calcite gradually decreased, and the recovery rate of scheelite remained stable. When the dosage of EA was 10 mg/L, the recovery rate of calcite dropped to 4.11%, and that of scheelite stabilized at 83.94%. The results showed that the interaction between EA agent and calcite was selectively inhibited.

3.2. Adsorption capacity test

Utilizing formula (2) alongside the adsorption capacity test, the adsorption density of EA on both scheelite and calcite surfaces was computed, as depicted in Fig. 6. The concentration of EA ranged from 2 to 10 mg/L. As the EA concentration increased, its adsorption density on scheelite surfaces ranged from 0.04 mg/m^2 to 0.26 mg/m^2. Conversely, on calcite surfaces, there was a significant rise in EA adsorption density, ranging from 0.12 mg/m^2 to 0.63 mg/m^2, indicating a distinct difference compared to its adsorption on scheelite surfaces. These results suggest selective adsorption of EA on calcite surfaces, consistent with the findings of the microflotation test.

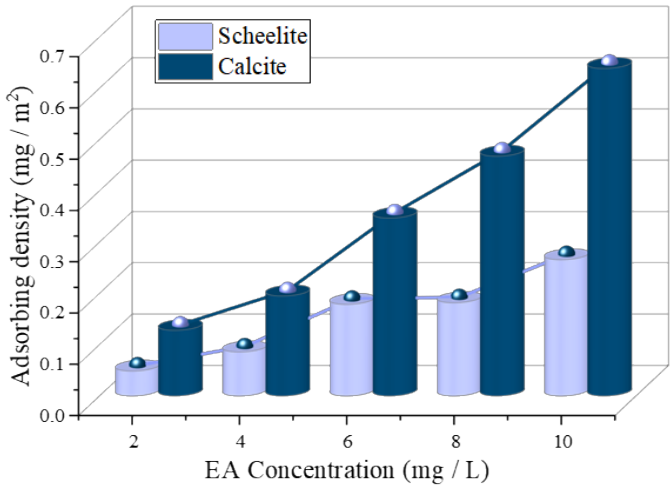

Fig. 6. Relationship between the adsorption density of scheelite and calcite and the EA and EA concentrations

3.3. Zeta potential test

Fig. 7 illustrates the effects of different chemical regimes on the zeta potentials of scheelite and calcite at different pH values. As shown in Fig. 7 (A), the zeta potential of scheelite decreased with increasing pH, while the isoelectric point of scheelite did not increase, and both values were negative (Wei et al., 2020; Dai et al., 2024). At pH = 8, the zeta potential after adding EA to scheelite shows a negative shift of approximately 13 mV, which may be because EA contains many negatively charged hydroxyl groups, and a trace amount of EA can act on the surface of scheelite. In the presence of NaOL, the potential is notably shifted further to the negative side (–44.7 mV), whereas it stands at 10.1 mV when only EA is added. This indicates that NaOL can continue to effectively interact with the scheelite surface even after treatment with EA.

Fig. 7 (B) shows that the isoelectric point (IEP) of the original calcite is about 9.5 at pH, which is consistent with previous literature (Gao et al., 2022; Liu et al., 2021). After interaction with EA, zeta potential moves to negative value. At pH = 8, zeta potential decreased from 9.4 mV to -14.6 mV, with a significant negative shift of 24 mV. These findings suggest significant EA adsorption on the calcite surface. Additionally, when both EA and NaOL are introduced after EA treatment, the potential change in calcite is minimal. This observation implies that a considerable portion of EA interacts with calcite, impeding further NaOL adsorption and consequently inhibiting calcite flotation. Thus, EA demonstrates effective selective inhibition.

3.4. FTIR analysis

Fig. 8 shows the infrared spectra of minerals under varying chemical conditions. In the scheelite raw ore spectrum shown in Fig. 8 (A), the W-O tensile and bending vibrations are evident at 805.8 cm^{-1} (Jiao

et al., 2023). Interaction with EA does not result in new absorption peaks on scheelite. However, after the reaction of EA and NaOL, two new absorption peaks emerge at 2923.1 cm^{-1} and 2856.3 cm^{-1}, corresponding to the absorption peaks of methylene and methyl in NaOL (Bai et al., 2023). This indicates that the interaction between NaOL and scheelite surface is less affected by EA. In Fig. 8 (B), the spectrum of raw calcite ore reveals a C-O tensile vibration peak at 1413.2 cm^{-1}, along with two deformation vibration characteristic peaks at 877.8 cm^{-1} and 703.9 cm^{-1} (Chen et al., 2017). Upon reaction with EA, a new benzene ring absorption peak appeared at 1621.0 cm^{-1} (Bai et al., 2023; Li et al., 2023). It's a good indication that there's a chemical interaction between the two. However, in the spectra after the action of EA and NaOL, there is no characteristic absorption peak of NaOL except the characteristic peak (micro-displacement) at 1614.9 cm^{-1}. The results of FTIR analysis are in line with those of adsorption capacity, confirming the effective selective inhibition of calcite by EA.

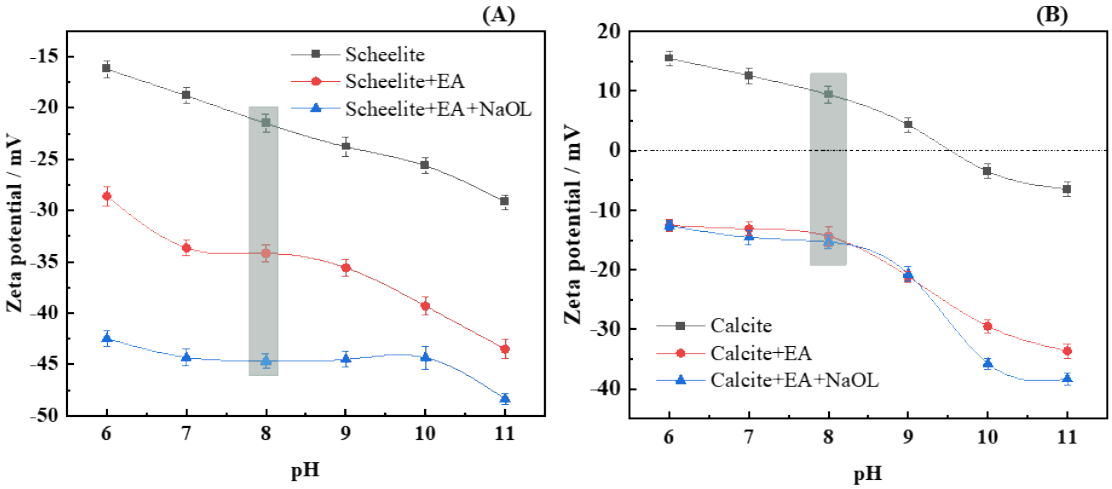

Fig. 7. Zeta potential of the mineral surface under different pH conditions

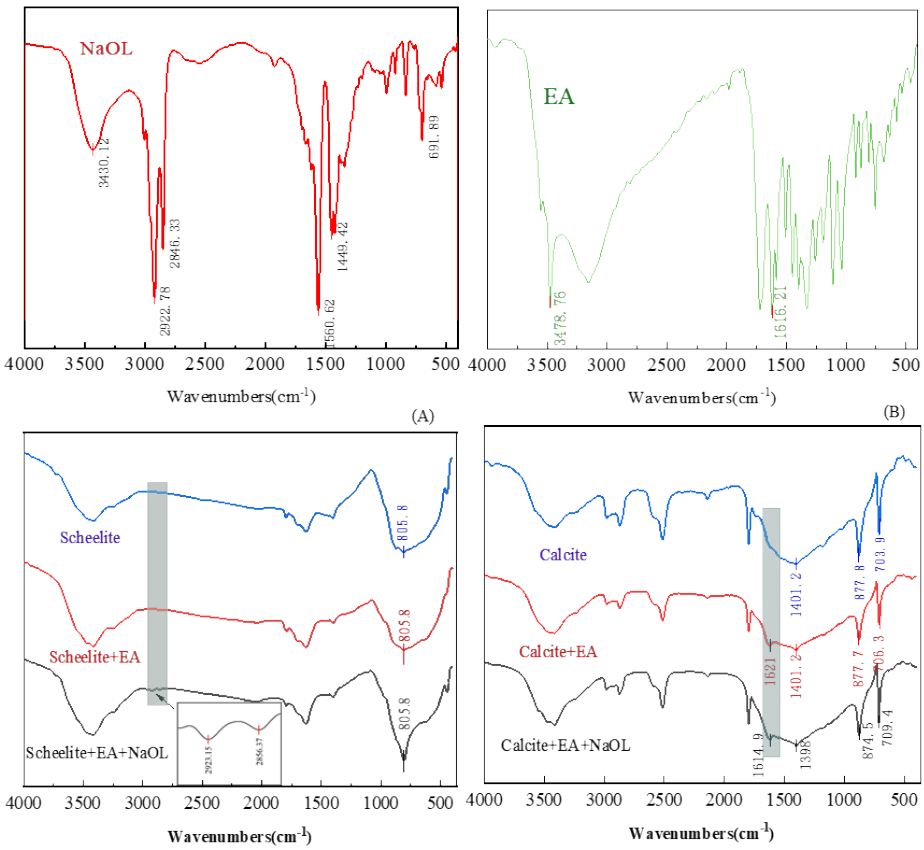

Fig. 8. Infrared spectra of scheelite and calcite under different chemical regimes

3.5. XPS analysis

XPS analysis provided deeper insights into how the depressant EA adsorbs onto calcite. The C 1s and O 1s spectra before and after the interaction of EA with calcite are displayed in Fig. 9. In Fig. 9 (A), calcite exhibits distinct CO_3^{2-} peaks at 289.29 eV, along with additional peaks at 284.78 eV attributed to carbon oxide contaminants on the calcite surface. Post EA treatment, in addition to the CO_3^{2-} peak, a new C-OH characteristic peak appears at 286.28 eV (Zhang et al., 2024). The suggesting chemisorption of EA onto the calcite surface. Fig. 9 (B) shows the high-resolution spectrum of calcite O 1s, revealing separate peaks at 531.18 eV and 532.41 eV, corresponding to CO_3^{2-} and carbon oxide contamination (Jiao et al., 2023). Following EA treatment, a new peak appears at 531.34 eV, attributed to the -COOR functional group in EA (Jiao et al., 2019; Gao et al., 2019). This further supports the occurrence of chemisorbed EA on the calcite surface.

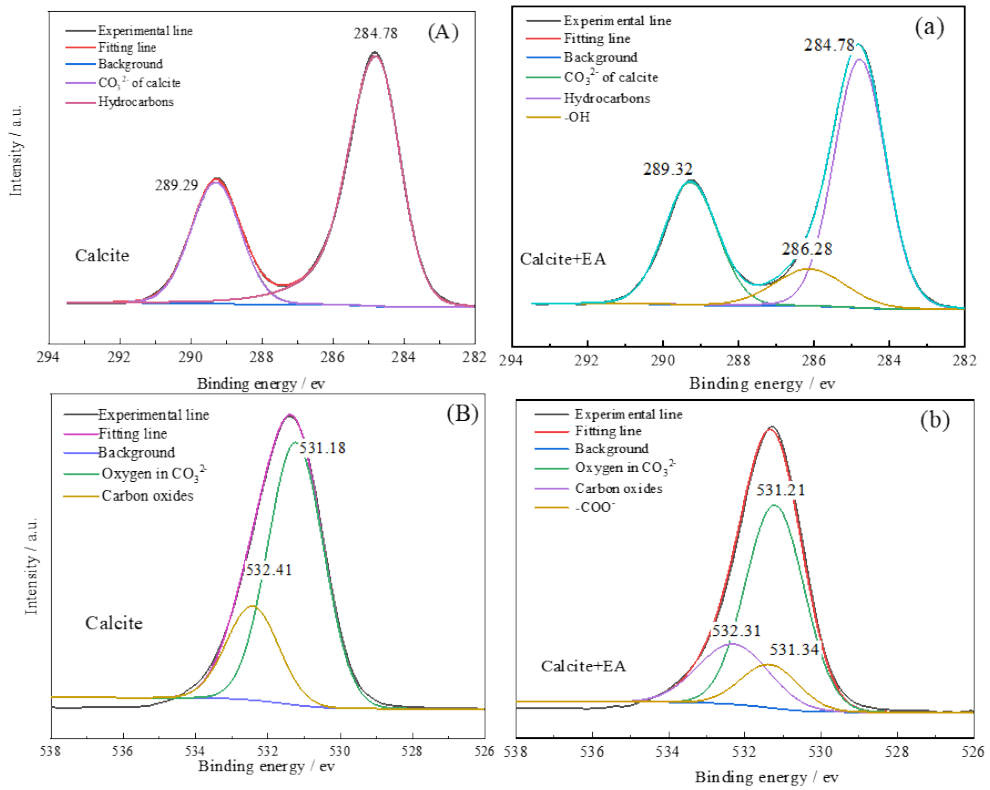

Fig. 9. Fitting peaks of C 1s (A) and O 1s (B) on calcite surfaces before and after EA

As depicted in Fig. 10, the high-resolution spectra of scheelite reveal C 1s and O 1s peaks. In Fig. 10 (A), a peak at 284.87 eV appears in the C 1s spectrum of scheelite, attributed to carbon oxide (Deng et al., 2018). Following the reaction of EA with scheelite, the C 1s spectrum of scheelite remains largely unchanged. In Fig. 10 (B), the O 1s spectrum of scheelite exhibits two separate peaks at 530.30 eV and 531.98 eV, attributed to scheelite itself, Ca-O, and carbon oxides (Cui et al., 2020). After the EA reaction, the peak displacement of scheelite is 0.2 eV (instrument detection error ≤ 0.4 eV), indicating that the mineral surface environment has not undergone significant changes following the interaction between tungsten ore and EA.

Additionally, the relative concentration changes of the corresponding atoms after the interaction of the agent with the mineral are shown in Table 3. Upon the interaction of scheelite with EA, there is a 0.65% increase in the relative carbon content on the scheelite surface, while calcium and oxygen elements decrease by 0.27% and 0.49%, respectively. Conversely, following the interaction of EA with calcite, the relative carbon content increases by 1.33%, surpassing that on the surface of scheelite. This elevation is attributed to EA containing a substantial amount of carbon adsorbed on the calcite surface, leading to the observed increase in carbon concentration. Meanwhile, the relative content of calcium and oxygen decreases by 0.84% and 1.17%, respectively. The atomic concentration of calcite surface changes more than scheelite, EA treatment changes the chemical composition of calcite surface.

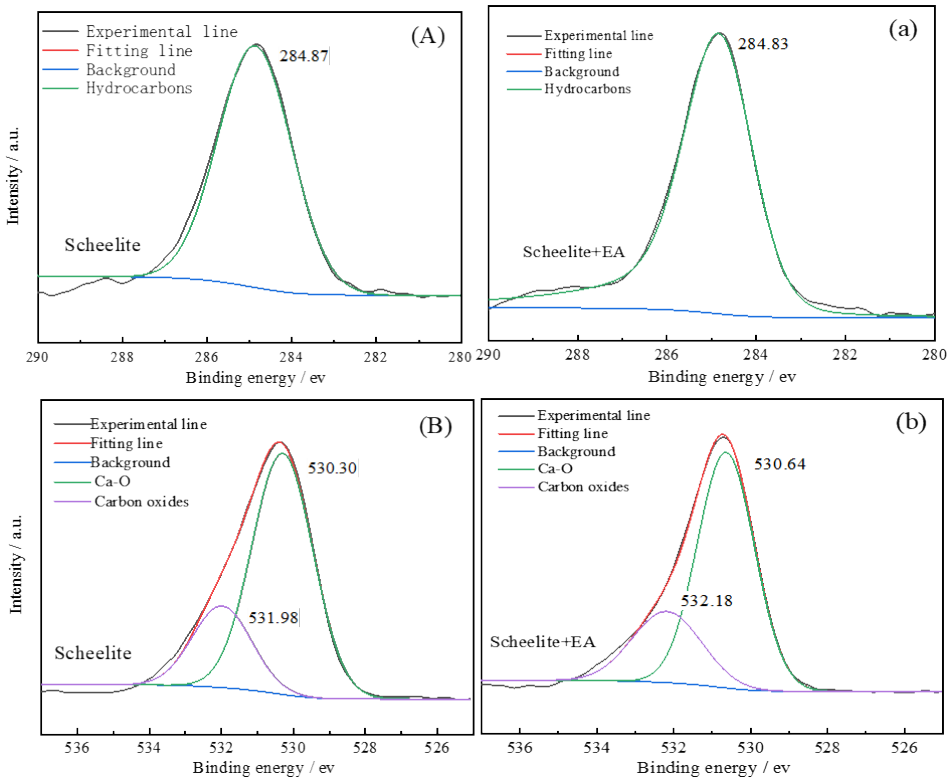

Fig. 10. Fitting peaks of C 1s (A) and O 1s (B) on scheelite surfaces before and after EA

Table 3. Atomic concentrations on the scheelite and calcite surfaces

Samples	Atomic concentration (%)		
	C1s	O1s	Ca2p
scheelite	30.23	48.95	9.35
scheelite+EA	30.88	48.68	8.86
calcite	50.65	42.40	12.26
calcite+EA	51.98	41.56	11.09

3.6. Contact angle measurement

Fig. 11 presents a diagram illustrating the contact angles of calcite and scheelite under different agent regimes. Fig. 11 (a-c) depict the behavior of the calcite mineral. Initially, untreated calcite exhibits a surface contact angle of 45.52°. Upon the addition of the EA agent, this angle decreases notably to 29.45°. Subsequent addition of NaOL results in minimal change in the contact angle, which only increases to 32.50°. This indicates that calcite impedes further NaOL adsorption after EA adsorption. Fig. 11 (d-f) illustrate the change in the contact angle of scheelite. Initially, the raw ore exhibits a contact angle of 51.38°, which decreases to 44.63° after interaction with EA. Despite this, scheelite retains effective NaOL adsorption capability, with the contact angle increasing significantly to 75.37°. These contact angle measurements correspond well with the flotation results.

3.7. AFM analysis

AFM provides direct insight into how minerals' surfaces are affected by flotation agents. Fig. 12 presents the two-dimensional and three-dimensional morphological changes of calcite (a, b) and scheelite (c, d) before and after interacting with EA. Surface roughness is evaluated using R_q (root mean square value) and Ra (arithmetic mean value) (Li et al., 2024). Fig. 12 (a) displays the smooth surface of untreated calcite ore (R_q = 4.73 nm, R_a = 3.35 nm), while Fig. 12 (b) shows the topography of calcite after EA interaction. Here, R_q increases significantly to 17.3 nm and Ra to 13.7 nm, indicating a denser adsorption layer formed by EA on the calcite surface. Both 2D and 3D images confirm this. Conversely, Fig. 12 (c, d) depict minimal surface changes in scheelite before and after EA treatment, with R_q ranging from 2.43

nm to 3.03 nm and Ra from 1.92 nm to 2.11 nm. These results suggest that EA adsorption on scheelite post-interaction is not pronounced, which is consistent with the adsorption capacity and contact angle test outcomes.

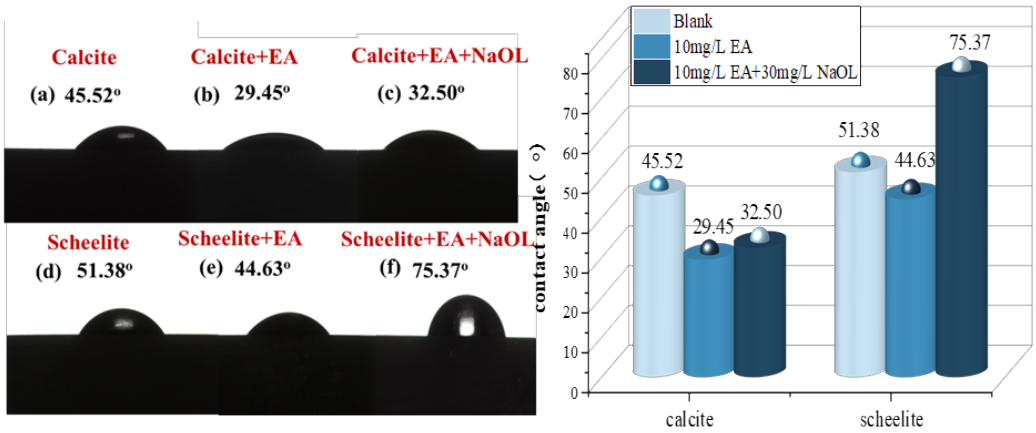

Fig. 11. Photographs and data of the contact angles of (a-c) calcite and (d-f) scheelite under different condition

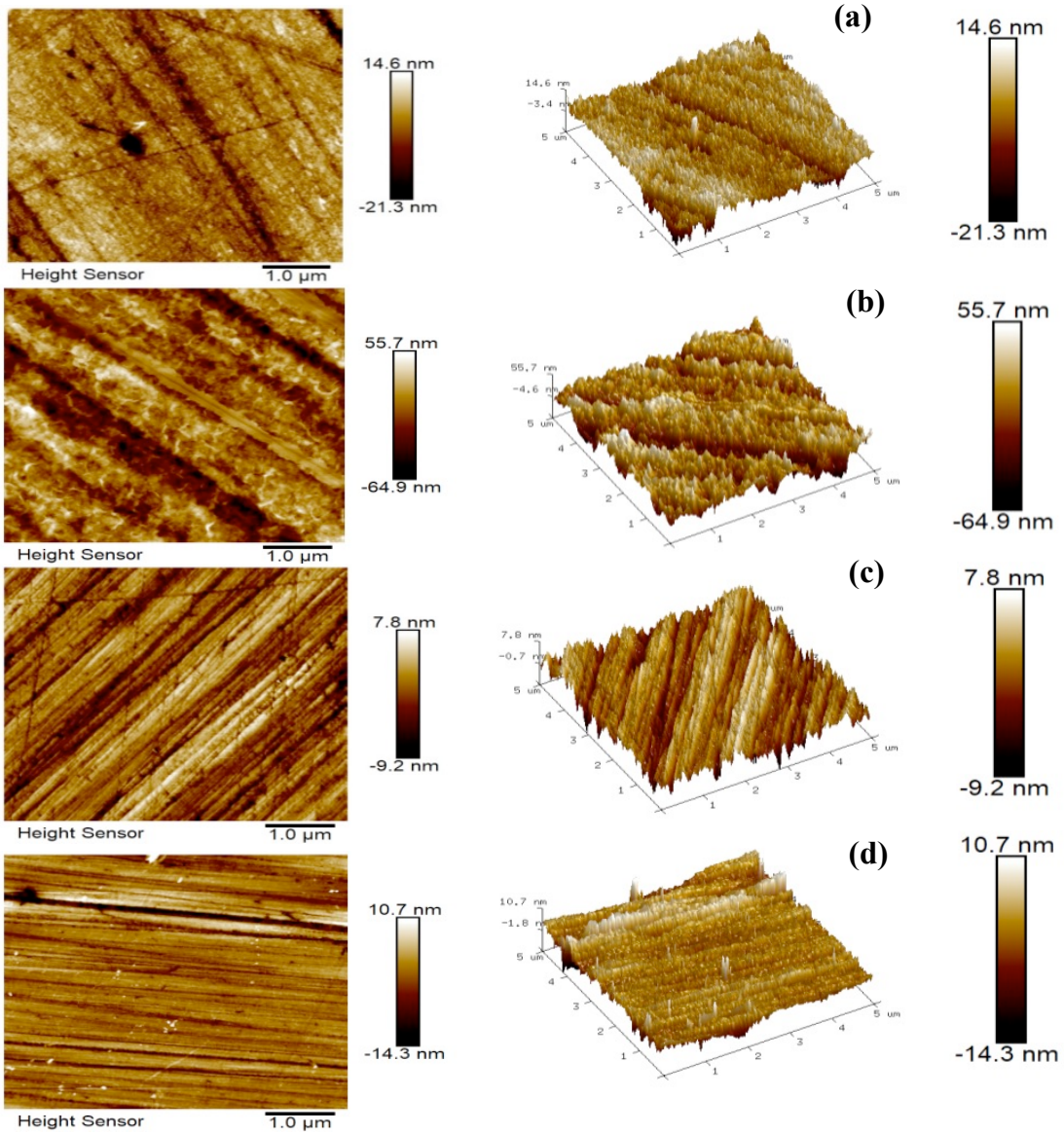

Fig. 12. AFM images of minerals before and after EA treatment

3.8. DFT simulation analysis

The EA molecule comprises two end groups: -OH and -COOR, which exhibit a propensity for strong complexation with metal ions (Dalvi et al., 2017). Fig. 13 depicts the electrostatic potential distribution of EA molecules. Positive and negative electrostatic potentials reflect the molecular electrical distribution to a certain extent. From the Fig. 11, it is evident that the negative electric area is concentrated near the oxygen atoms of C=O and -OH. Therefore, these groups are chosen for adsorption simulation with calcium atoms on the surface of calcite (Taheri et al., 2022; Politzer et al., 1985).

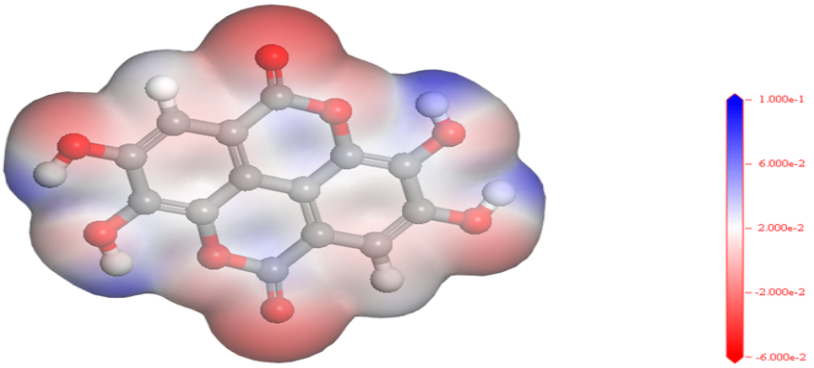

Fig. 13. Electrostatic potential distribution diagram of the EA

Calcite exhibits a higher surface calcium density and a shorter calcium-oxygen bond length compared to scheelite (Gao et al., 2016; Gao et al. 2013; Gao et al., 2018). Consequently, calcite is more reactive. In Fig. 14 the adsorption Settings of the agent on the surface of calcite (104) are determined after geometric optimization by DFT. It is suggested that EA may be bonded to Ca by hydroxyl oxygen and two lactone oxygen. Their negative adsorption energy means that the adsorption is spontaneous, as shown in Table 4. Fig. 14 (A) shows the adsorption of the -OH group on the surface of calcite (104), forming A Ca-O bond with a length of 2.400 A. This length is less than the sum of the covalent radii of Ca and O atoms (2.47 A) (Guan et al., 2024b). With a population of 0.12 and an adsorption energy of -109.90 kJ/mol (Table 4), this bond should be the most stable. Fig. 14 (B) describes the adsorption of -COOR groups on the surface of calcite. The length of CA-O bond is 2.305 A, the population of the bond is 0.16, and the adsorption energy is -102.41 kJ/mol (Table 4). The O atom in C=O forms a bond interaction with the Ca atom on the surface of calcite.

Fig. 14 (C) depicts the -OH and -COOR groups forming two Ca-O bond adsorption configurations with calcite simultaneously. In this setup, the length of the O1-Ca1 keys is 2.697A and the population is 0.06. The length of the O2-Ca2 bond is 2.429 A, the population is 0.15, and the adsorption energy of the two groups is -95.03 kJ/mol. The EA hydroxyl and carbonyl oxygen bonds form a Ca-O-C structure on the surface of calcite (104), consistent with previous results for XPS, and this specific interaction leads to selective inhibition of calcite.

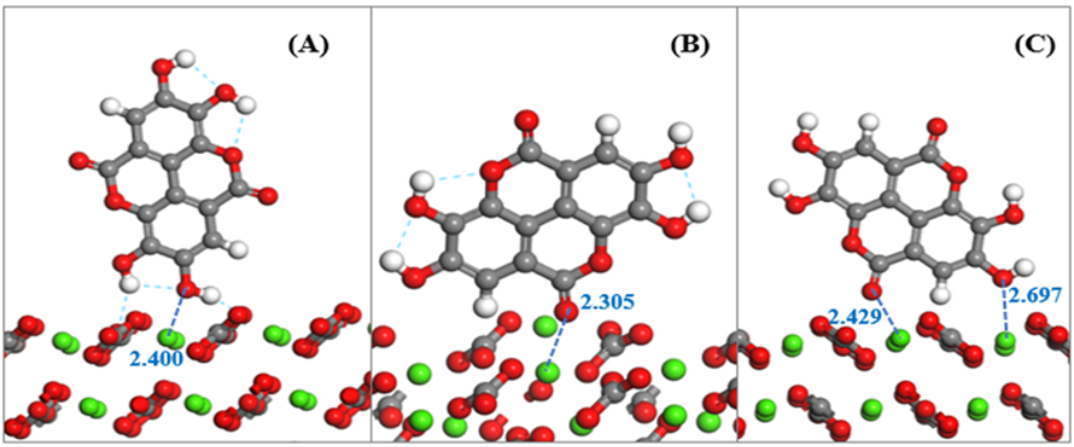

Fig. 14. Adsorption model of EA and calcite (104)

Table 4. Adsorbed atoms and their binding properties.

Model	Bond Type	Bond Populations	Bond length/Å	Eads/(kJ/mol)
Calcite + EA (-OH)	O1-Ca1	0.12	2.3995	-109.90
Calcite + EA (C=O)	O2-Ca2	0.16	2.30485	-102.41
Calcite + EA (-OH, C=O)	O1-Ca1	0.06	2.69712	-95.03
	O2-Ca2	0.15	2.42689	

4. Conclusions

In this investigation, ellagic acid (EA) demonstrates significant efficacy as a depressant for the separation and flotation of scheelite and calcite, with the main findings summarized as follows:

(1) Microflotation test outcomes indicate that at a pH of 8, with a sodium oleate concentration of 30 mg/L and an EA concentration of 8 mg/L, the recovery rate for scheelite reaches 89.35%, whereas for calcite it is merely 6.22%. EA selectively inhibits calcite while allowing scheelite to sustain a high recovery rate.

(2) Various tests, including adsorption capacity, contact angle, AFM, and Zeta potential reveal that EA exhibits low adsorbability on the scheelite surface, which does not interfere with the adsorption of the collector NaOL; thus, maintaining good hydrophobicity on the scheelite surface. In contrast, EA strongly adheres to the calcite surface, obstructing NaOL adsorption and preserving the hydrophilicity of the calcite surface.

(3) FTIR and XPS analyses demonstrate that following interaction with EA, the characteristic peak in the infrared spectrum of calcite is attributed to EA, whereas the peak for scheelite corresponds solely to NaOL. This supports the selectivity in flotation separation of the minerals. XPS analysis reveals that EA primarily binds to the calcite surface through chemisorption of -OH and -COOR groups, with no significant alteration observed on the scheelite surface.

(4) The DFT simulation analysis corroborated the experimental findings, revealing that EA primarily attaches to the surface of calcite (104) through the chemisorption of -OH and C=O groups. The calcium atom in calcite serves as the active binding site for EA. This interaction enhances the microenvironmental polarity of calcite while diminishing its hydrophobic properties. As shown in Table 5. Comparison of the effect of new organic inhibitors, compared with previous studies, ultra-low concentration EA provides a new way to improve the flotation separation efficiency of scheelite and reduce the amount of chemical agents. This method offers a green and sustainable solution for scheelite flotation. Additionally, it provides a theoretical foundation and experimental support for investigating the interaction of EA with other minerals, optimizing its structure and properties, and developing more innovative inhibitors.

Table 5. Comparison of the effect of new organic inhibitors of calcite.

Reagent	Dosage	Calcite Recovery rate (%)	Flotation Recovery Difference (%)	Reference
Pectin	20 mg/L	4.56%	66.45%	Jiao et al., 2019
Dextrin	200 mg/L	38%	55%	Wei et al., 2023b
Citric acid	5.0×10^{-4}mol/L	20.55%	62.2%	Yao et al., 2023
Tartaric acid/Fe^{3+}	5.0×10^{-4}mol/L	9.4%	74.35%	Zhang et al., 2018
Ellagic acid	**8 mg/L**	**6.22%**	**89.35%**	**–**

Acknowledgements

This work was supported by the National Natural Science Foundation of China [grant numbers 52164022].

References

AGRAWAL, O.D., Y.A. KULKARNI, 2020. *Mini-review of analytical methods used in quantification of ellagic acid,* Reviews in Analytical Chemistry, 39, 31-44.

AI, G., C. LIU, W. ZHANG, 2018. *Utilization of sodium humate as selective depressants for calcite on the flotation of scheelite*, Separation Science and Technology, 53, 2136-2143.

BAI, S., J. LI, Y. BI, J. YUAN, S. WEN, Z. DING, 2023. *Adsorption of sodium oleate at the microfine hematite/aqueous solution interface and its consequences for flotation*, International Journal of Mining Science and Technology, 33, 105-113.

CHEN, W., Q. FENG, G. ZHANG, Q. YANG, C. ZHANG, 2017. *The effect of sodium alginate on the flotation separation of scheelite from calcite and fluorite*, Minerals Engineering, 113, 1-7.

CUI, Y., F. JIAO, Q. WEI, X. WANG, L. DONG, 2020. *Flotation separation of fluorite from calcite using sulfonated lignite as depressant,* Separation and Purification Technology, 242, 116698.

DAI, L., J. LIU, D. LI, J. HAO, H. GAO, 2024. *A new insight on a novel auxiliary collector 4-MBA synergize with BHA to enhance flotation of scheelite*, Separation and Purification Technology, 346, 127412.

DALVI, L.T., D.C. MOREIRA, R. ANDRADE JR, J. GINANI, A. ALONSO, M. HERMES-LIMA, 2017. *Ellagic acid inhibits iron-mediated free radical formation*, Spectrochimica Acta Part A: Molecular and Biomolecular Spectroscopy, 173, 910-917.

DENG, R., X. YANG, Y. HU, J. KU, W. ZUO, Y. MA, 2018. E*ffect of Fe(II) as assistant depressant on flotation separation of scheelite from calcite*, Minerals Engineering, 118, 133-140.

DONG, L., L. QIAO, Q. ZHENG, P. SHEN, W. QIN, F. JIAO, D. LIU, 2023. *Enhanced adsorption of citric acid at the calcite surface by adding copper ions: Flotation separation of scheelite from calcite*, Colloids and Surfaces A: Physicochemical and Engineering Aspects, 663, 131036.

DONG, L., F. JIAO, W. QIN, Q. WEI, 2021. *Utilization of iron ions to improve the depressive efficiency of tartaric acid on the flotation separation of scheelite from calcite*, Minerals Engineering, 168, 106925.

DONG, L., F. JIAO, W. QIN, W. LIU, 2019. *Selective flotation of scheelite from calcite using xanthan gum as depressant*, Minerals Engineering, 138, 14-23.

GAO, Z., J. DENG, W. SUN, J. WANG, Y. LIU, F. XU, Q. WANG, 2022. *Selective Flotation of Scheelite from Calcite Using a Novel Reagent Scheme,* Mineral Processing and Extractive Metallurgy Review, 43, 137-149.

GAO, Z., Z. WANG, J. CHANG, L. CHEN, D. WU, F. XU, X. WANG, K. JIANG, 2019. *Micelles directed preparation of ternary cobalt hydroxide carbonate-nickel hydroxide-reduced graphene oxide composite porous nanowire arrays with superior faradic capacitance performance*, Journal of Colloid and Interface Science, 534, 563-573.

GAO, Z., Y. HU, W. SUN, J.W. DRELICH, 2016. S*urface-charge anisotropy of scheelite crystals*, Langmuir, 32, 6282-6288.

GAO, Z.-Y. S. WEI, Y.-H. HU, X.-W. LIU, 2013. *Surface energies and appearances of commonly exposed surfaces of scheelite crystal,* Transactions of Nonferrous Metals Society of China, 23, 2147-2152.

GAO, Y., Z. GAO, W. SUN, Z. YIN, J. WANG, Y. HU, 2018. *Adsorption of a novel reagent scheme on scheelite and calcite causing an effective flotation separation*, Journal of Colloid and Interface Science, 512, 39-46.

GUAN, Z., K. LU, Y. ZHANG, H. YANG, X. LI, 2022. S*tudy of the Effect of Manganese Ion Addition Points on the Separation of Scheelite and Calcite by Sodium Silicate*, Materials, 15, 4699.

GUAN, Z., R. LIAO, Q. ZUO, Y. WU, Y. ZHANG, S. WEN, 2024a. *Mechanistic analysis and validation of an efficient novel inhibitor for scheelite and calcite flotation separation: A DFT and MD simulation study*, Applied Surface Science, 662, 160146.

GUAN, Z., Y. ZHANG, S. WEN, Y. WU, X. LI, X. LI, 2024b. M*n-SS as a novel depressant of the flotation process of scheelite and calcite: Role and mechanism*, Colloids and Surfaces A: Physicochemical and Engineering Aspects, 686, 133443.

JIAO, F., W. LI, X. WANG, C. YANG, Z. ZHANG, L. FU, W. QIN, 2023. *Application of EDTMPS as a novel calcite depressant in scheelite flotation*, International Journal of Mining Science and Technology, 33, 639-647.

JIAO, F., L. DONG, W. QIN, W. LIU, C. HU, 2019. F*lotation separation of scheelite from calcite using pectin as depressant*, Minerals Engineering, 136, 120-128.

LI, X., H. HE, Y. ZHANG, Y. WU, Z. GUAN, 2023. *Flotation separation of scheelite from calcite using baicalin as a depressant,* Colloids and Surfaces A: Physicochemical and Engineering Aspects, 675, 132006.

LI, X., Y. ZHANG, H. HE, Y. WU, D. WU, Z. GUAN, 2024. F*lotation separation of scheelite from calcite using luteolin as a novel depressant*, International Journal of Minerals, Metallurgy and Materials, 31, 462-472.

LIU, C., C. NI, J. YAO, Z. CHANG, Z. WANG, G. ZENG, X. LUO, L. YANG, Z. REN, P. SHAO, L. DUAN, T. LIU, M. XIAO, 2021. *Hydroxypropyl amine surfactant: A novel flotation collector for efficient separation of scheelite from*

calcite, Minerals Engineering, 167, 106898.

PENG, T., L. TAO, J. WANG, L. DONG, W. JIA, F. WANG, J. HU, Z. GAO, 2024. *Selective flotation separation of scheelite from calcite using hexamethylenediamine tetramethylene phosphonic acid as a novel depressant*, Journal of molecular liquids, 402, 124569.

POLITZER, P., P.R. LAURENCE, K. JAYASURIYA, 1985. *Molecular electrostatic potentials: an effective tool for the elucidation of biochemical phenomena*, Environmental health perspectives, 61, 191-202.

RÍOS, J.-L., R.M. GINER, M. MARÍN, M.C. RECIO, 2018. *A pharmacological update of ellagic acid*, Planta medica, 84, 1068-1093.

TAHERI, B., F. REZAEI, N. SHADJOU, A. HASSANZADEH, 2022. *A molecular analysis on nitrile-based collectors and their application to chalcopyrite flotation*, Minerals Engineering, 186, 107763.

WANG, J., J. BAI, W. YIN, X. LIANG, 2018. F*lotation separation of scheelite from calcite using carboxyl methyl cellulose as depressant*, Minerals Engineering, 127, 329-333.

WEI, Z., W SUN, P WANG, H HAN, D LIU. 2023. *The structure analysis of metal-organic complex collector: From single crystal, liquid phase, to solid/liquid interface*. Journal of Molecular Liquids, 382, 122029.

WEI, Z., W SUN, H HAN, Y XING, X GUI , 2023a. *Molecular design of multiple ligand metal–organic framework (ML-MOF) collectors for efficient flotation separation of minerals*. .Separation & Purification Technology, 328, 125048.

WEI, Z., W SUN, H HAN, X GUI, Y XING. 2023. F*lotation chemistry of scheelite and its practice: A comprehensive review*. Minerals Engineering, 204, 108404.

WEI, Z., J. FU, H. HAN, W. SUN, T. YUE, L. WANG, L. SUN, 2020. *A Highly Selective Reagent Scheme for Scheelite Flotation: Polyaspartic Acid and Pb–BHA Complexes*, Minerals, 10, 561.

YAO, W., Y. WU, M. LI, R. CUI, J. LI, Z. YANG, Y. FU, Z. PAN, D. WANG, M. ZHANG, 2023. E*xploring Dextrin as an Eco-Friendly Depressant for Selective Flotation Separation of Scheelite and Calcite Minerals*, Mineral Processing and Extractive Metallurgy Review, 143-152.

YI, H., F. JIA, Y. ZHAO, W. WANG, S. SONG, H. LI, C. LIU, 2018. *Surface wettability of montmorillonite (0 0 1) surface as affected by surface charge and exchangeable cations: a molecular dynamic study*, Applied Surface Science, 459, 148-154.

ZHANG, Y., R. CHEN, Y. LI, Y. WANG, X. LUO, 2018. *Flotation separation of scheelite from calcite using sodium polyacrylate as depressant*, Physicochemical Problems of Mineral Processing, 54, 505-516.

ZHU, W., L. DONG, F. JIAO, W. QIN, Q. WEI, 2019. *Use of sodium hexametaphosphate and citric acid Mixture as depressant in the flotation separation of scheelite from calcite*, Minerals, 9, 560.